

KATARZYNA STANIENDA-PILECKI*[#]**CARBONATE MINERALS WITH MAGNESIUM IN TRIASSIC TEREBRATULA LIMESTONE
IN THE TERM OF LIMESTONE WITH MAGNESIUM APPLICATION AS A SORBENT
IN DESULFURIZATION OF FLUE GASES****MINERAŁY WĘGLANOWE ZAWIERAJĄCE MAGNEZ W WAPIENIACH TRIASOWYCH WARSTW
TEREBRATULOWYCH W ASPEKTCIE ZASTOSOWANIA WAPIENI Z MAGNEZEM
JAKO SORBENTU W PROCESIE ODSIARCZANIA SPALIN**

This article presents the results of studies of Triassic (Muschelkalk) carbonate rock samples of the Terebratula Beds taken from the area of the Polish part of the Germanic Basin. It is the area of Opole Silesia. The rocks were studied in the term of possibility of limestone with magnesium application in desulfurization of flue gases executed in power plants. Characteristic features of especially carbonate phases including magnesium-low-Mg calcite, high-Mg calcite, dolomite and huntite were presented in the article. They were studied to show that the presence of carbonate phases with magnesium, especially high-Mg calcite makes the desulfurization process more effective. Selected rock samples were examined using a microscope with polarized, transmitted light, X-ray diffraction, microprobe measurements and FTIR spectroscopy. The results of studies show a domination of low magnesium calcite in the limestones of the Terebratula Beds. In some samples dolomite and lower amounts of high-Mg calcite occurred. Moreover, huntite was identified. The studies were very important, because carbonate phases like high-Mg calcite and huntite which occurred in rocks of the Triassic Terebratula Beds were not investigated in details by other scientists but they presence in limestone sorbent could influence the effectiveness of desulfurization process.

Keywords: limestone, carbonates with magnesium, sorbent, desulfurization

W artykule zaprezentowano wyniki badań wapieni triasowych (wapienia muszlowego) warstw terebratulowych. Próbki pobrano w obszarze Śląska Opolskiego (polska część zbiornika germańskiego). Próbki poddano badaniom w celu określenia możliwości zastosowania wapieni z magnezem w procesie odsiarczania gazów spalinowych, stosowanym w zakładach energetycznych. Charakterystyczne własności faz węglanowych, w szczególności tych zawierających magnez, takich jak kalcyt niskomagnezowy, kalcyt wysokomagnezowy, dolomit i huntyt, przedstawiono w niniejszym

* SILESIAN UNIVERSITY OF TECHNOLOGY, FACULTY OF MINING AND GEOLOGY, DEPARTMENT OF APPLIED GEOLOGY, 2 AKADEMICKA STR., 44-100 GLIWICE, POLAND

[#] Corresponding author: Katarzyna.Stanienda-Pilecki@polsl.pl

artykule. Badania wykonano w celu wykazania, że obecność faz węglanowych zawierających magnez, w szczególności wysokomagnezowy kalcyt, wpływają na zwiększenie efektywności procesu odsiarczania spalin. Próbkę wapieni poddano badaniom, obejmującym m.in. analizę mikroskopową w świetle przechodzącym, dyfraktometrię rentgenowską, badania w mikroobszarach oraz spektroskopię w podczerwieni FTIR. Wyniki badań wskazują na dominację niskomagnezowego kalcytu w wapieniach warstw terebratulowych. W niektórych próbkach zidentyfikowano dolomit i mniejsze ilości kalcytu wysokomagnezowego. Ponadto oznaczono również huntyt. Przeprowadzenie badań było bardzo istotne, ponieważ fazy węglanowe takie jak kalcyt wysokomagnezowy i huntyt, które zidentyfikowano w wapieniach triasowych warstw terebratulowych nie były wcześniej, przez innych naukowców szczegółowo badane, a ich obecność w sorbencie węglanowym może wpływać na polepszenie efektywności procesu odsiarczania spalin.

Słowa kluczowe: wapień, fazy węglanowe z magnezem, sorbent, odsiarczanie

1. Introduction

Middle Triassic (Muschelkalk) limestones from the area of Opole Silesia in Poland are deposits of the Eastern Part of the epicontinental Germanic Basin (Niedźwiedzki, 2000; Szulc, 2000). In analyzed area many limestone quarries are situated. In lots of them Triassic limestones are mined. They are used in different branches of industry also in desulfurization of flue gases in power plants. It is very important process because nowadays most energy is still obtained from brown coal and hard coal. During coal combustion sulfur oxides are emanated and are emitted into the atmosphere. Desulfurization of flue gases allow to reduce the emission of sulfur oxides into the atmosphere. Limestone sorbent including carbonate phases rich in magnesium could be applied in dry desulfurization, mainly in modern method using Fluidized Bed Reactor. Rocks of the Terebratula Beds were chosen as a subject of this article because a detailed analysis of carbonate phases rich in magnesium in these rocks in the term of these rocks application in desulfurization had not been done before. Diversification of Lower Muschelkalk deposits with content of Mg and Ca, which was observed in limestones of Gogolin Beds, Górażdże Beds, Terebratula Beds and Karchowice Beds (Bodzioch, 2005; Stanienda, 2011, 2013a, b; Szulc, 2000) is the effect of sedimentation conditions in the Germanic Basin. The Terebratula Beds were forming during the sea transgression. The results of previous research on carbonate phases rich in magnesium in Muschelkalk rocks of the Polish part of the Germanic Basin were very general. They show that these rocks are mainly built of low-Mg calcite, high-Mg calcite and dolomite (Bodzioch, 2005; Stanienda, 2011, 2013a, b; Szulc, 2000). The knowledge of the type of mineral phases including magnesium and their content in investigated rocks are very important for establishing the possibility of application limestone rich in magnesium carbonate phases as a sorbent in desulfurization of flue gases. Usually the limestone with the content of $MgO < 2\%$ is used however the presence of magnesium in carbonate sorbent could make a desulfurization process more effective. Carbonate phases rich in Mg such as high-Mg calcite and huntite rarely occur in Triassic rocks. High-Mg calcite which occurs in limestone of Terebratula Beds is an unstable carbonate phase in comparison to low-Mg calcite as it may lose its Mg in time and alter to low-Mg calcite (Boggs, 2010; Zhang & Dave, 2000). Huntite which was also identified in analyzed rocks occurs in sedimentary rocks in the deposits of the vadose zone (Deelman, 2011). The results of researches allow to confirm the theory which indicate that the presence of Mg in carbonate sorbent make desulfurization process more effective.

2. Materials and methods

2.1. Field investigation

The samples were collected in the area of Opole Silesia in the following quarries: Strzelce Opolskie (samples SO1, SO2, SO3, SO4, SO5, SO6, SO9, SO10, SO27, SO28, SO29, SO30), Szymiszów (samples S1, S2, S3, S4, S5, S6, S7, S8, S9) and in the area of St. Anne's Mountain in the park which surrounds the Amphitheatre (samples SA10, SA11, SA12) (Pl. 1) (Stanienda, 2013a). At the bottom Kamionek Marl Member is situated, above – St. Anne's Mountain Encrinite Member and at the top – Chelm Coguina Member. The total thickness of the Terebratula Beds in the Strzelce Opolskie quarry varies in the range 12-14 m, in the area of St. Anne's Mountain it is 13.8 m (Niedźwiedzki, 2000). The outcrop of Muschelkalk in the Szymiszów quarry includes only the Terebratula Beds. The thickness of this formation there is about 2.5 m. The samples were taken from all members (Tab. 1).

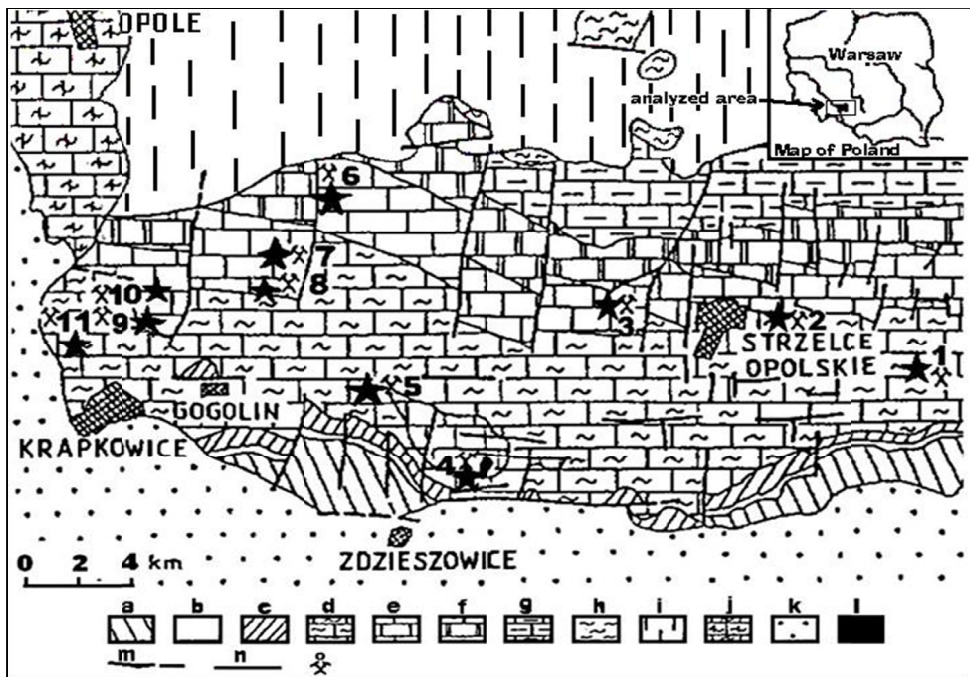


Plate 1. Geological map of the central part of Opole Silesia (according to Niedźwiedzki R., 2000, modified by Stanienda K., 2013a – determination of area for researches, marking the places of sampling)
 a – greywackes of Lower Carboniferous; b – sandstones and mudstones of Middle Buntsandstein; c – limestones, dolomites and marls of Upper Buntstandstein (Roethian); d – limestones and marls of Gogolin Beds; e – limestones of Górażdże Beds, Terebratula Beds and Karchowice Beds; f – dolomites of Jemielnice Beds; g – limestones and dolomites of Rybna beds and Boruszowice Beds; h – claystones, mudstones and sandstones of Keuper; i – claystones of Rhaetian; j – sandstones, marls and limestones of Upper Cretaceous; k – sandstones, clays and gravels of Neogene; l – Tertiary basalts; m – faults; n – stratigraphic boundaries; o – important quarries: 1 – Błotnica Strzelecka; 2 – Dziewkowice; 3 – Szymiszów; 4 – St. Anne's Mountain and Wysoka; 5 – Ligota Dolna and Kamienna; 6 – Tarnów Opolski; 7 – Kamień Śląski; 8 – Górażdże and Kamionek; 9 – Malnia; 10 – Chorula; 11 – Rogów Opolski; * areas of sampling

TABLE 1

Results of sampling

Unit	The number of samples	Member description
Kamionek Marl Member	Five samples: all from Strzelce Opolskie quarry- SO9, SO27, SO28, SO29, SO30)	The unit is built of very thin-bedded marls and also thin-bedded limestone with a grainstone layer which is situated in the lower part of the Kamionek Marl Member (Bodzioch, 2005). The thickness of the unit in the Strzelce Opolskie quarry is 3.5 m. Sample SO27 comes from the lower part of the Kamionek Marl Member, samples SO28 and SO29 – from the middle part and samples SO9 and SO30 – form the upper part.
St. Anne's Mountain Encrinite Member	Seven samples: two from the area of St. Anne's Mountain- SA10, SA11, five from the Strzelce Opolskie quarry- SO1, SO2, SO3, SO4, SO10)	The lower part of the St. Anne's Mountain Encrinite Member is built of pelitic and crumpled limestones, the upper part contains medium-bedded crinoidal packstone and grainstone (Bodzioch, 2005). The thickness of this unit varies in range from 1.60 to 2.00 m (Niedźwiedzki, 2000). The samples from the area of St. Anne's Mountain were collected from the upper part of the member, 40 cm under the top of the member. Samples SO1 and SO3 come from the lower part of the St. Anne's Mountain Encrinite Member, samples SO2 and SO10 – from the middle part and sample SO4 – from the upper part.
Chelm Coquina Member	Twelve samples: one in the area of St. Anne's Mountain- SA12, two in the Strzelce Opolskie quarry-SO5, SO6, nine- in the Szymiszów quarry- S1, S2, S3, S4, S5, S6, S7, S8, S9)	The Chelm Coquina Member is built of two complexes of inter-bedded layers of terebratulids coquina and crumpled limestone. They are separated by a wavy-crumpled limestone complex (Bodzioch, 2005). The total thickness of this member fluctuates from 7.85 to 8.60 m. In the Szymiszów quarry, it is possible to observe only the outcrop of the Chelm Coquina Member. The thickness of the strata in this outcrop is 2.5 m. In the area of Saint Anne Mountain sample SA12 was collected from the middle part of the member. Sample SO5 of the Strzelce Opolskie quarry comes from the lower part of the member and sample SO6 – from the upper part. All samples of the Szymiszów quarry come from the upper part of the Coquinoid Limestone of Chelm.

2.2. Laboratory investigation

All samples were described using a petrographic microscope with polarized transmitted light. The microscopic analysis was executed in Institute of Applied Geology of the Silesian University of Technology, using the Opton Axioplan Universal Microscope with Image Analyser K300, produced by Zeiss. Six samples were studied applying X-ray diffraction: 3 from the Strzelce Opolskie quarry (SO1, SO28, SO30), 2 – from the Szymiszów quarry (S2, S5), one from the area of St. Anne's Mountain (SA10). The X-ray diffraction was carried out at the Institute of Applied Geology of the Silesian University of Technology, using the HZG4 diffractometer with the application of a copper lamp with nickel screen and the following analysis conditions: voltage 35kV, intensity 18mA. Microprobe measurements examined 3 samples: SO1 (from Strzelce Opolskie quarry), S2 (from Szymiszów quarry), SA12 (from the area of St. Anne's Mountain). The studies were carried out at the Institute of Non-ferrous Metals in Gliwice. The analyses were conducted using the techniques of X-ray microanalysis EPMA, with the application of the X-ray

microanalyser JXA-8230 manufactured by JOEL. The examinations were performed on polished sections which were sputtered with a carbon coat. The analysis with the application of WDS spectrometers and EDS spectrometer was carried out in microareas of the samples. The WDS method was applied to conduct quantitative analyses in microareas with a size of $60 \mu\text{m} \times 45 \mu\text{m}$ (magn. $2000\times$) for selected points having different chemical compositions. The contents of the following chemical elements were determined: Mg, Al, Si, K, Ca, Mn, Fe, Sr, Ba, O and C. The X-ray map of the microarea was made using the EDS spectrometer with the magnification of $500\times$ (imaging area $240 \mu\text{m} \times 170 \mu\text{m}$) as well as element spectra at the measurement points. The content of the following elements was determined: O, C, Mg, Ca and Fe. The Fourier analysis in the infrared (FTIR) was applied to investigate 6 samples: 2 from Strzelce Opolskie quarry (SO1, SO28), 2 – from the area of St. Anne's Mountain (SA10, SA12), 2 – from Szymiszów quarry (S2, S8). The researches studies were carried out at the Institute of Geological Sciences of the Jagiellonian University using the Fourier spectrometer FTS 135 BioRad. The spectra were elaborated using the software provided by the manufacturer (Bio-Rad Sadtler Division 1981-1993).

3. Results of study

3.1. General macroscopic description of samples

All collected samples were analyzed according to their texture and structure features. Photographs of representative samples are presented in Plate 2. Generally, the rocks of the Terebratula Beds do not present a big variability in the mineral composition (Stanienda, 2013a). The samples description was done according to the standards presented by Boggs (2010) and Flügel (2004).

Rocks of Kamionek Marl Member (Pl. 2 – A, B) are represented by samples SO9, SO27, SO28, SO29, SO30. The limestones form medium or thin beds. The limestones are usually dark grey (Pl. 2B) or dark beige (Pl. 2A) in colour. Their texture is usually micritic (sample SO9, SO27, SO28) (Pl. 2B) very seldom bioclastic in some areas of rock (samples SO29, SO30) (Pl. 3A) and structure disorderly unoriented, porous (samples SO27, SO28, SO29, SO30) (Pl. 2 – A, B), in some samples massive (sample SO9). In rocks of this unit very seldom is possible to observe fossils, terebratulids or fragments of crinoids – stem plates (Pl. 2B). The rocks are mainly built of calcite groundmass. Moreover, iron minerals occur (iron oxides, sometimes pyrite).

Rocks of St. Anne's Mountain Member (Pl. 2 – C, D) build the middle unit of analyzed profile. The rocks form thin, medium or thick beds. Some of them are limestones (samples SA10, SA11, SO1, SO2, SO3, SO4), others – dolomitic limestones (sample SO10). They are yellowish, cream or grey in colour. Their texture is bioclastic (samples SO3, SO4, SA10, SO1, SA11), in some samples micritic (sample SO2, SO10), structure – massive (samples SA10, SA11, SO2, SO4, SO10), in some samples porous (samples SO1, SO3). In rocks of this unit fossils of terebratulids and crinoids – stem plates were observed. The rocks are mainly built of calcite, moreover dolomite and iron minerals occur (iron oxides, sometimes pyrite).

Rocks of Chelm Coquina Member (Pl. 2 – E, F) build the top unit of Terebratula Beds. The rocks usually form medium size beds. They are usually grey marl limestones (samples SO5, SO6, S1, S2, S3, S4, S5, S6, S7, SA12) or dolomitic limestones (samples S8, S9). They are dark grey, sometimes dark brown (an effect of strong weathering) in colour. Their texture is usually micritic (samples S1, S3, S4, S5, S6, S7, S8, S9, SA12) or bioclastic (samples SO5, S2) and structure – unoriented, porous. In some samples pores are filled with sparry calcite. In some

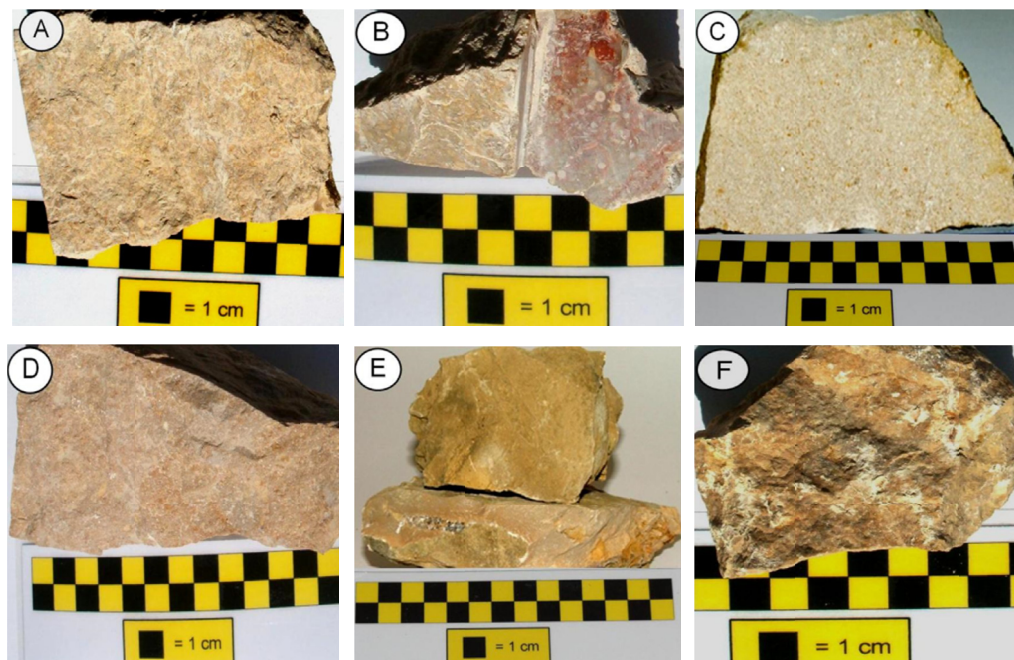


Plate 2. Examples of limestone samples of Terebratula Beds.

A – Rock sample SO27 from the Kamionek Marl Member; B – Rock sample SO29 from the Kamionek Marl Member; C – Rock sample SA10 from the St. Anne’s Mountain Encrinite Member (Stanienda et al., 2011); D – Rock sample SO10 from the St. Anne’s Mountain Encrinite Member; E – Rock sample SA12 from the Chelm Coquina Member (Stanienda et al., 2011); F – Rock sample S2 from the Chelm Coquina Member

samples it was possible to observe concentrations of terebratulids fossils which size ranges from 2 cm up to 15 cm. The rocks are mainly built of calcite, moreover dolomite and iron minerals occur (iron oxides, pyrite).

3.2. Results of microscopic analysis

Results of microscopic analysis allowed to distinguish only two carbonate phases: calcite and dolomite. Non-carbonate minerals include: quartz, chalcedony, iron minerals (goethite, hematite, pyrite) and in some samples clay minerals. The higher content of non-carbonate minerals was observed in the rocks from the Kamionek Marl Member and an increased content of crinoids in the St. Anne’s Mountain Encrinite Member (Pl. 3). A microscopic characteristic of analyzed rocks broadens the data which have been published before (Stanienda, 2013a). The samples description was done according to the standards presented by Boggs (2010) and Flügel (2004).

Rocks of *Kamionek Marl Member* present sparry or microsparry texture, sometimes bioclastic one. There is a very small amount of allochems (bioclasts) in this type of rocks. Single bioclasts are crinoids stem plates and shells of terebratulids (samples SO9, SO28). Allochems are built of the micritic calcite, sometimes of sparry crystals. The areas between bioclasts are filled with the granular or mosaic cement built of spar, microspar or micrite (samples SO27, SO28). Occasionally, bladed, syntaxial cement was observed (samples SO28) (Boggs, 2010). In some

samples bioclasts are distributed chaotically in matrix (sample SO29). Some samples are built only of sparry groundmass (matrix) which is built of sparry crystals different in size (0.02-0.1 mm) and in shape (irregular, oval, sometimes rhombohedral) (samples SO27, SO28, SO30). In some areas of rocks microsparry groundmass (grain size from 5-30 μm) is visible and in others- palisade neomorphic sparite, coming from recrystallization of *periostracum* (primary aragonitic), which sometimes surrounds bioclasts (samples SO28) (Pl. 3D). In some samples (SO28, SO29, SO30) it is possible to observe sparry veins and bunches filled with coarse-grained calcite (Pl. 3E). It is also possible to notice parts of dissolved shells filled with sparry calcite. In bigger calcite crystals rhombohedral cleavage is visible (sample SO30) (Pl. 3E). It is the secondary calcite (pseudospar) formed by aggradation and recrystallization of primary micritic crystals during diagenesis. The rocks which present microsparitic texture (sample SO9) are built of microspar or spar (pseudospar). In the groundmass veins and bunches filled with sparry calcite occur (Pl. 3C). The rocks are mainly built of calcite. Its crystals are different in size (from micritic to sparry). In some samples (SO28, SO29, SO30) also dolomite was identified. It forms sparry, rhombohedral crystals. Among non-carbonates chalcedony (sample SO27) and quartz (samples SO9, SO28) dominate. Also iron minerals were observed. They are dispersed in groundmass, sometimes form

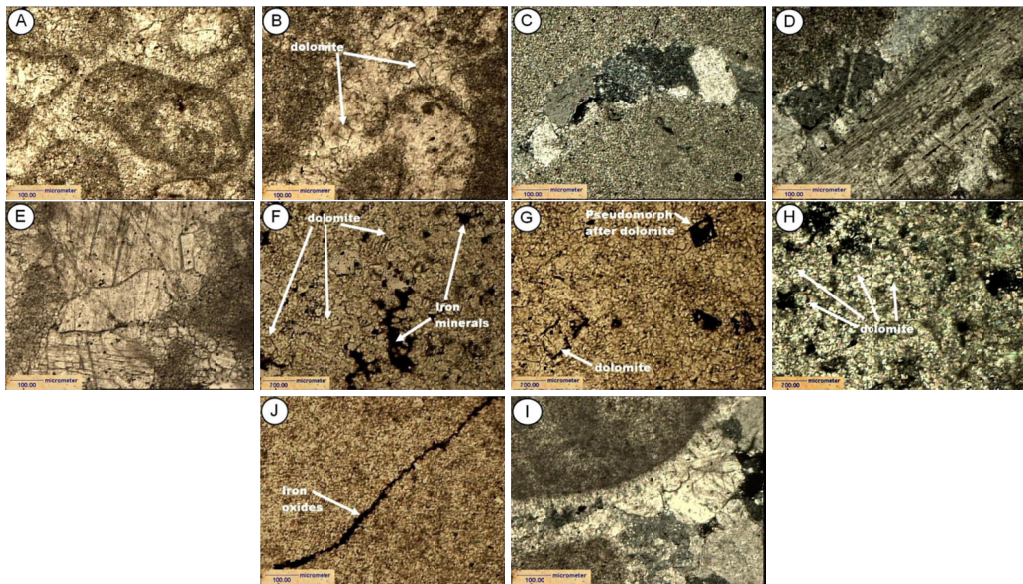


Plate 3. Microscopic images of selected limestone samples.

A – sample SO1 – bioclasts in spar mass in some areas of rock microspar. 1N; B – sample SO3 – part of dissolved shell filled with spar calcite and rhombohedral dolomite in microspar mass. 1N; C – sample SO9 – shell filled with a blocky spar in microsparry rock mass. XN; D – sample SO28 – terebratulid Brachiopod (*Coenothyris* probably) surrounded by palisade sparite formed by recrystallization of *periostracum*. XN; E – sample SO30 – spar calcite with visible cleavage in microspar mass. 1N; F – sample S2 – rhombohedral dolomite crystals and aggregates of iron minerals, iron oxides and/or pyrite in some areas of rock. 1N; G – sample S4 – rhombohedral dolomite crystals in limestone built of spar; pseudomorphs after dolomite, some of them filled with iron compounds. 1N; H – sample S5 – rhombohedral dolomite crystals in limestone built of spar. XN; I – sample SA10 – palisade neomorphic sparite surrounds bioclast. 1N; J – sample SA12 – limestone built of microspar; a dissolution seam or crack filled with iron minerals (goethite, hematite, pyrite). 1N

aggregates or fill up stylolites, dissolution seams or cracks. Opaque crystals could be treated as pyrite. According to a microscopic analysis, the rocks from this unit could be classified as mudstone or as wackstone.

In rocks of *St. Anne's Mountain Encrinite Member* (samples SA10, SA11, SO1, SO3, SO4, SO10) a lots of allochems (bioclasts) were observed, mainly crinoids stem plates, shells of teribratulids (sample SO1), foraminifera, peloids and aggregates. The texture of rocks is bioclastic. The presence of crinoids stem plates could indicate the shelf environment (Flügel, 2004). Some allochems are built of sparry calcite, others – of microsparry or micritic crystals, which also represent calcite phases. In the areas of bioclasts contact or in pores between bioclasts the matrix was noticed (samples SA10, SO1, SO3) (Pl. 3A). It forms granular or mosaic cement (Boggs, 2010) built of sparry or microsparry crystals different in size (samples SA10, SO1, SO3), in some areas of samples – micritic ones (sample SO1, SO3, SO10). In some areas of rocks palisade neomorphic sparite was observed (samples SA10, SO1, SO3) (Pl. 3I). In samples SO3 and SO4 it is possible to find parts of dissolved shells filled with sparry calcite and rhombohedral dolomite (Pl. 3B). In some calcite crystals rhombohedral cleavage is visible (sample SO4). It is the second generation calcite formed during diagenesis (pseudospar). The matrix which predominates in rocks is normally built of microspar (sample SO2). A characteristic feature of these rocks is presence of veins and bunches filled with sparry calcite which are arranged disorderly in the matrix. Calcite phases predominate in the rocks of member. It forms crystals different in size (from micritic to sparry). Moreover sparry, euhedral, rhombohedral dolomite crystals were observed (samples SA10, SO1, SO3, SO4, SO10). It was also possible to detect pseudomorphs after dolomite (sample SO10). Some pseudomorphs are filled with iron oxides. Among non-carbonate phases iron oxides dominate. They filled dissolution seams, cracks (sample SA11), dolomite pseudomorphs (sample SO10), stylolites (sample SO3), sometimes they are dispersed in groundmass or form concentrations. Opaque crystals could be treated as pyrite. According to a microscopic analysis the samples of this unit could be classified as packstone, grainstone seldom as floatstone.

Rocks of *Chelm Coquina Member* present sparry or microsparry texture, seldom bioclastic one. Rocks with bioclastic texture built shell limestone which forms inter-layers in marl limestones. The rocks are built of microspar groundmass (matrix), in some areas of rock- spar or micrite- orthochems, composed of crystals different in size and shape (from 0.02 to 0.1 mm). The matrix is built of calcite and dolomite. Calcite crystals ranges from micrite to spar. Dolomite forms sparry crystals. Also in these rocks it is possible to find bunches and veins filled with sparry calcite. Its crystals are bigger in size than crystals (more than 0,1 mm) which build the matrix (samples S1, S7, S8, SA12). Dolomite which occurs in sparry groundmass forms euhedral, rhomboherdral in shape crystals (samples S1, S2, S4, S5, S8, S9). In some samples pseudomorphs after dolomite were detected (samples S2, S4, S9). They are filled with iron oxides. In rocks with bioclastic texture (samples SO5, S2, S7) allochems (bioclasts) predominate- mostly shells, foraminifera fossils, sometimes crinoids stem plates. They are built of micritic calcite, seldom – the sparry one (sample S2). It is also possible to observe aggregates of micritic calcite. Some bioclasts are surrounded by a micritic cover. The areas of the bioclasts contact are filled with sparry (0.02-0.1 mm), granular or mosaic cement (sample S2) (Boggs, 2010). In some areas of rocks palisade neomorphic sparite is visible. Among carbonate minerals calcite phases dominate but dolomite is also present (samples S1, S2, S4, S5, S8, S9) (Pl. 3- F, G, H). Non-carbonates are represented by quartz (sample S4), chalcedony (samples S1, S2, S3, S4, S7, S8) and iron minerals (samples S1, S2, S4, S5, S7, S8, S9, SA12). Iron minerals are dispersed in rock mass, sometimes they form aggregates

tograms which did not belong to low-Mg calcite and in samples – S2 and S5 (Pl. 4 – E, F) to dolomite shows that these lines present lattice parameters proportionally lower than interplane values changes d_{hkl} of diffraction lines characteristic for low-Mg calcite. These diffraction lines are typical for high-Mg calcite. The d_{104} value of high-Mg calcite depends on $MgCO_3$ content. The value of $d_{104} - 2.988 \text{ \AA}$ is typical for high-Mg calcite with content of $MgCO_3 - 16.3 \text{ mol \%}$, the value of $d_{104} - 2.972 \text{ \AA}$ for content of $MgCO_3 - 22.5 \text{ mol \%}$ (Zhang & Dave, 2000). If the content of $MgCO_3$ rises, the value of d_{104} drops. Unstable calcite phases could also present the value of $d_{104} - 2.964 \text{ \AA}$ (Smyth & Ahrens, 1997). High-Mg calcite was identified mainly on the basis of d_{104} value in samples S2, S5 (Pl. 4 – E, F). In diffractograms of samples S2 and S5 also other diffraction lines typical for this phase were determined. High-Mg calcite occur in rocks of Chelm Coquina Member. Dolomite was identified in samples SO30, SA10 and S5. So as dolomite occurred in the rocks of all members of the Terebratula Beds. Huntite was identified only in one sample – S5 (Pl. 4F), on the basis of diffraction line of the highest intensity – 2.83 \AA and also on the basis of three other diffraction lines of lower intensity (Yavuz et al., 2006; <http://rruff.info/Huntite>).

Huntite like high-Mg calcite occurred only in rocks of Chelm Coquina Member. Also quartz (samples SO28 – Pl. 4A, SO30 – Pl. 4B, SO1 – Pl. 4C, S2 – Pl. 4E, S5 – Pl. 4F), ankerite (samples SO28 – Pl. 4A, SO30 – Pl. 4B, SO1 – Pl. 4C), orthoclase (samples SO28 – Pl. 4A, S5 – Pl. 4F) and illite (sample S2 – Pl. 4E) were identified. However illite was determined only on the basis of one diffraction line, so its presence in the sample S2 is doubtful.

3.4. Results of microprobe measurements

Sample SO1 – limestone from St. Anne’s Mountain Encrinite Member

In *microarea 1 of the SO1 sample*, in the area of groundmass, the EDS analysis was carried out. The selected specimen fragment is built of the calcite of light grey in colour and carbonate phase enriched in Mg which forms euhedral, rhombohedral crystals dark grey in colour (Pl. 5). The areas white in colour are built of alumina and silica phases. The results of a chemical analysis (Tab. 2, Pl. 6) show that elements values measured there are average values determined for the entire microarea. The results indicate a domination of low-Mg calcite there. But carbonate phases enriched in Mg, silicates, aluminosilicates and iron minerals also occur.

In *the second microarea of sample SO1*, inside of groundmass the WDS analysis was carried out (Pl. 7) (Stanienda, 2013a). The chemical composition of the sample, determined by means of penetration, at the selected points of this microarea (Tab. 3) show that the carbonate phase presented here is characterized by a diversified chemical composition due to the presence of Ca and Mg. A slight enrichment in Mg was identified around dark grey areas which take up around 10% of the microarea surface (Pl. 7). The results of a chemical analysis indicate the domination of low-Mg calcite. The content of Mg in low-Mg calcite varies in points from 0.03 to 0.24%, the content of Ca from 40.55 to 41.07%. At all points the presence of Fe was determined, at some points- small amounts of Ba, Sr and Mn (Tab. 3). The presence of Sr and Ba points out to the occurrence of aragonite in the original carbonate sediment.

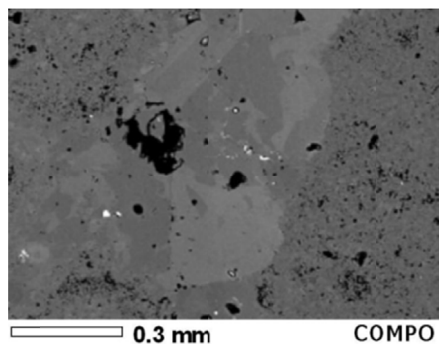


Plate 5. BSE first image of a sample SO1

TABLE 2

Microprobe chemical analyses of a sample SO1

Chemical formula	% mass
C	8.87
O	26.52
Mg	0.12
Al	0.13
Si	0.23
Ca	63.79
Fe	0.34
Total	100.00

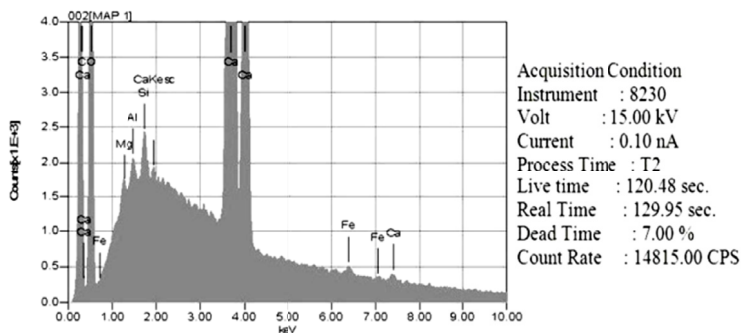


Plate 6. Spectrum of chemical elements in the first microarea of a sample SO1

TABLE 3

Microprobe chemical analyses in second microarea of sample SO1 (Stanienda, 2013a)

Point number	Type of chemical element [%mass]											Total
	O	C	Mg	Si	Al	Ca	K	Ba	Sr	Fe	Mn	
1	53.91	4.89	0.24	0.00	0.00	40.55	0.00	0.00	0.04	0.36	0.01	100.00
2	53.91	4.87	0.19	0.00	0.00	40.66	0.00	0.00	0.00	0.35	0.02	100.00
3	53.01	5.55	0.24	0.00	0.00	40.77	0.00	0.02	0.04	0.36	0.01	100.00
4	52.32	6.28	0.19	0.00	0.00	40.84	0.00	0.03	0.00	0.32	0.02	100.00
5	52.31	6.73	0.06	0.00	0.00	40.85	0.00	0.00	0.02	0.02	0.01	100.00
6	53.07	5.79	0.03	0.00	0.00	41.07	0.00	0.00	0.00	0.04	0.00	100.00

Sample S2 – limestone from Chelm Coquina Member

In *microarea 1 of the S2 sample* (in the area of groundmass) the EDS analysis was carried out. The selected specimen fragment is built mainly of the calcite phase grey in colour (Pl. 8). Areas white in colour are built of alumina and silica phases. The results of a chemical analysis (Tab. 4, Pl. 9) show that elements values measured there are average values determined for the entire microarea.

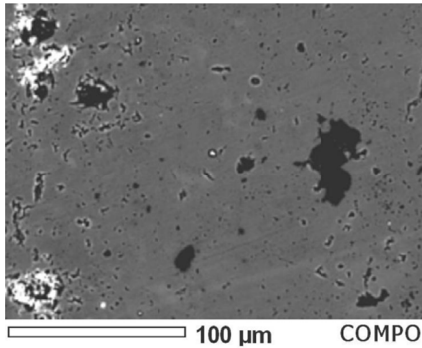


Plate 8. BSE first image of a sample S2. Magn. × 500

TABLE 4

Microprobe chemical analyses of a sample S2

Chemical formula	% mass
C	8.54
O	26.19
Mg	0.43
Al	0.11
Si	0.24
Ca	62.38
Fe	2.11
Total	100.00

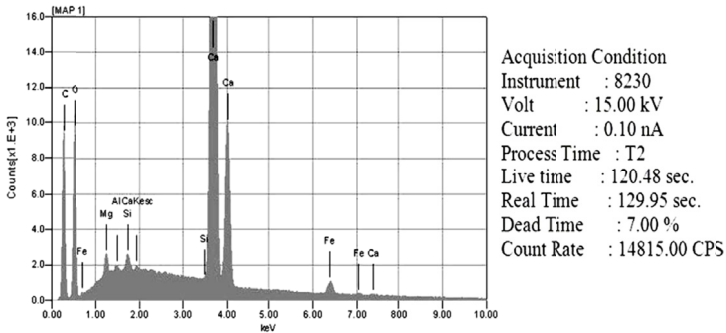


Plate 9. Spectrum of chemical elements in the first microarea of a sample S2

The results of the chemical analysis indicate a domination of low-Mg calcite. Moreover silicates and aluminosilicates occur. The results also indicate the enrichment of iron minerals in sample S2 (Pl. 9, Tab. 6).

In *the microareas 2 and 3 of sample S2*, inside of the groundmass, WDS analysis was carried out (Pl. 10, 11) (Stanienda, 2013a, b). The chemical composition of the sample, determined by means of penetration, at the selected points of these microareas (Tab. 5 and 6) show that the carbonate phase presented there is characterized by a diversified chemical composition due to the presence of Ca and Mg. The enrichment in Mg in *the microarea 2* (points 1, 2, 5) (Stanienda, 2013a) is identified around dark grey areas (Pl. 10). The phase enriched in Mg takes up around 20% of the microarea surface. The results of a chemical analysis carried out in microarea 2 indicate that two carbonate phases occur here: low-Mg calcite phase (Tab. 5 – points 3, 4), high-Mg calcite (Tab. 5 – points 2, 5) and dolomite (Tab. 5 – point 1). The content of Mg in low-Mg calcite phase varies in points from 0.20 to 0.30%, the content of Ca – from 41.00 to 41.50%. In high-Mg calcite the content of Mg varies in points from 7.10 to 10.70%, the content of Ca – from 26.30 to 38.40%. In dolomite phase the content of Mg presents value 13.20%, the content of Ca – 24.20%. At point 2 of microarea 2 (Tab. 5) the presence of Fe was determined, at point 3 – a small content of Sr. The presence of Sr points out to the occurrence of aragonite in

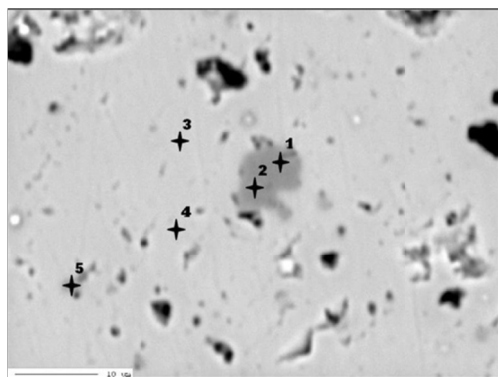


Plate 10. BSE second image of a sample S2 (Stanienda, 2013a).

Magn. $\times 2000$. Light grey – calcite, dark grey – carbonate phase rich in magnesium. 1-5 – points of chemical analysis

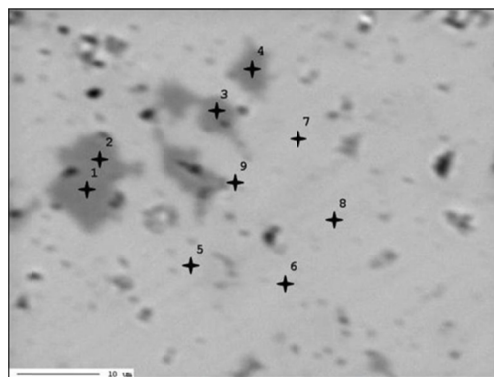


Plate 11. BSE third image of a sample S2 (Stanienda, 2013b).

Magn. $\times 500$. Light grey – calcite, dark grey – carbonate phase rich in magnesium, 1-9 – points of chemical analysis

the original carbonate sediment, which was transformed into low-Mg calcite during diagenesis. The enrichment in Mg in *the microarea 3* is identified around dark grey areas which take up around 35% of the microarea surface (Pl. 11) (Stanienda, 2013b). Light grey phase represents calcite. The results of a chemical analysis indicate the occurrence of two carbonate phases in this microarea: low-Mg calcite (Tab. 6 – points 5 to 9) and huntite (Tab. 6 – points 1 to 4).

The content of Mg in huntite phase varies from 14.6 to 16.2% in points, the content of Ca from 23.1 to 25.8%. The content of Mg in this phase is lower than the stoichiometric value typical for huntite, which varies from 20 to 21% Mg (33-34% MgO). The reduction of Mg in huntite could be caused by diagenetic processes. At all points (Tab. 8) the presence of iron was determined. At many points small amounts of Al and K were determined and at some points – Ba, Sr and Mn.

TABLE 5

Microprobe chemical analyses in second microarea of sample S2 (Stanienda, 2013a)

Point number	Type of chemical element [%mass]										Total	
	O	C	Mg	Si	Al	Ca	K	Ba	Sr	Fe		Mn
1	53.80	8.80	13.20	0.00	0.00	24.20	0.00	0.00	0.00	0.00	0.00	100.00
2	54.80	8.00	10.70	0.00	0.00	26.30	0.00	0.00	0.00	0.20	0.00	100.00
3	50.60	8.00	0.30	0.00	0.00	41.00	0.00	0.00	0.10	0.00	0.00	100.00
4	46.70	11.60	0.20	0.00	0.00	41.50	0.00	0.00	0.00	0.00	0.00	100.00
5	45.90	8.60	7.10	0.00	0.00	38.40	0.00	0.00	0.00	0.00	0.00	100.00

Sample SA12- limestone from Chelm Coquina Member

In *microarea 1 of SA12 sample*, inside of groundmass, the EDS analysis was carried out (Pl. 12). The selected specimen fragment of this limestone is built mainly of the calcite phase grey in colour. There are also some areas white in colour which indicate the occurrence of alu-

TABLE 6

Microprobe chemical analyses in third microarea of sample S2 (Stanienda, 2013b)

Point number	Type of chemical element [%mass]											Total
	O	C	Mg	Si	Al	Ca	K	Ba	Sr	Fe	Mn	
1	48.35	10.85	16.18	0.00	0.04	23.07	0.03	0.84	0.00	0.64	0.00	100.00
2	49.69	10.36	14.85	0.00	0.04	24.24	0.03	0.01	0.02	0.75	0.01	100.00
3	50.31	8.22	15.36	0.00	0.03	25.79	0.04	0.00	0.01	0.24	0.00	100.00
4	45.66	9.29	14.56	0.00	0.02	23.54	1.04	5.69	0.00	0.17	0.03	100.00
5	45.65	8.66	0.42	0.00	0.00	45.15	0.04	0.02	0.00	0.02	0.04	100.00
6	53.50	4.04	0.21	0.00	0.02	42.14	0.08	0.00	0.00	0.01	0.00	100.00
7	44.74	11.07	0.27	0.00	0.00	43.84	0.04	0.01	0.00	0.03	0.00	100.00
8	45.46	8.75	0.06	0.00	0.01	45.68	0.00	0.00	0.03	0.01	0.00	100.00
9	43.45	9.80	3.49	0.00	0.01	43.14	0.03	0.01	0.00	0.06	0.01	100.00

mina and silica phases. The results of a chemical analysis determined in this microarea (Tab. 7, Pl. 13) show that the elements values measured there are average values determined for the entire microarea. The results of the chemical show that in this rock low-Mg calcite dominates. The results indicate the enrichment of iron minerals in sample SA12.

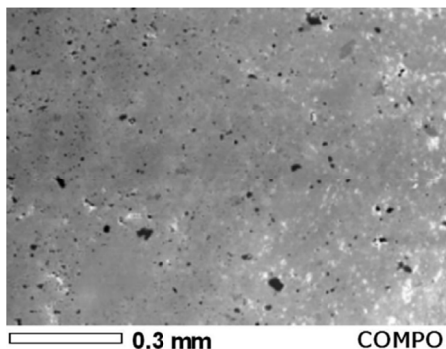
Plate 12. BSE first image of a sample SA12. Magn. $\times 100$

TABLE 7

Microprobe chemical analyses of a sample SA12

Chemical formula	% mass
C	11.84
O	35.56
Mg	0.33
Al	0.49
Si	1.43
Ca	50.14
Fe	0.21
Total	100.00

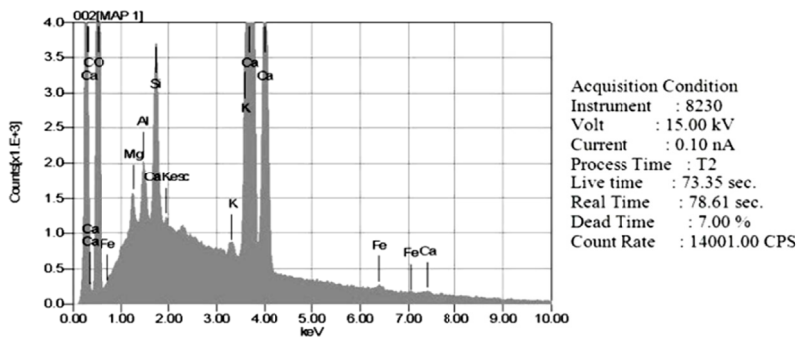


Plate 13. Spectrum of chemical elements in the first microarea of a sample SA12

In *the second microarea of sample SA12*, inside of groundmass, the WDS analysis was carried out (Pl. 14) (Stanienda, 2013a). The chemical composition of the sample, determined by means of penetration, at the selected points of this microarea (Tab. 8) show a domination of low-Mg calcite there. The results of a chemical analysis confirm the domination of this phase. The content of Mg in low-Mg calcite phase varies in points from 0.18 to 1.08%, the content of Ca from 36.94 to 41.66%. At all points of this microarea (Tab. 8) the presence of Si, Al, K and Fe were determined. It indicates the possibility of silicates and aluminosilicates occurrence. At some points small amounts of Ba, Sr and Mn were identified. The presence of Sr and Ba points out to the aragonite presence in the original carbonate sediment.

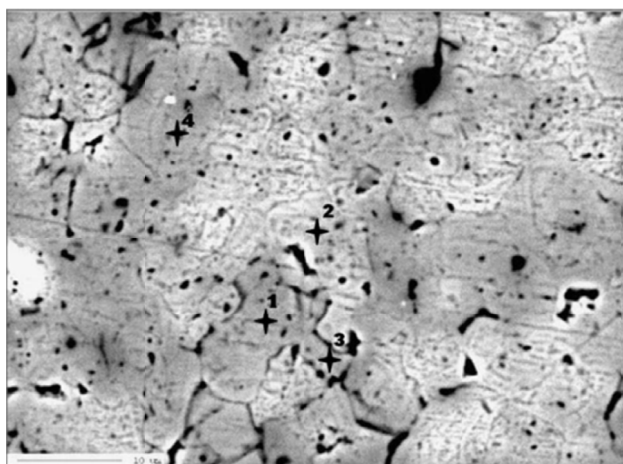


Plate 14. BSE second image of a sample SA12 (Stanienda, 2013a).
Magn. $\times 500$. Light grey – calcite, dark grey – carbonate phase rich in magnesium,
1-4 – points of chemical analysis

TABLE 8

Microprobe chemical analyses in third microarea of sample SA12 (Stanienda, 2013a)

Point number	Type of chemical element [%mass]											Total
	O	C	Mg	Si	Al	Ca	K	Ba	Sr	Fe	Mn	
1	48.12	8.90	1.08	0.04	0.06	41.66	0.02	0.00	0.04	0.06	0.02	100.00
2	51.88	9.00	0.94	0.63	0.27	36.94	0.05	0.08	0.08	0.13	0.00	100.00
3	49.72	8.43	0.25	0.13	0.19	40.91	0.03	0.00	0.00	0.34	0.00	100.00
4	50.33	10.78	0.18	0.32	0.12	37.91	0.04	0.00	0.12	0.20	0.00	100.00

3.5. Results of FTIR Spectroscopy

Results of the Fourier analysis in infrared show that in the investigated limestones low-Mg calcite dominates (Pl. 15) (Stanienda, 2013a, b). This phase was identified on the basis of the following infrared bands: $V_4 = 712 \text{ cm}^{-1}$, $V_2 = 847 \text{ cm}^{-1}$ and $V_2 = 874 \text{ cm}^{-1}$, V_3 – from 1420 cm^{-1} to 1422 cm^{-1} , $V_1 + V_4$ – from 1798 cm^{-1} to 1799 cm^{-1} , $V_1 + V_3$ – from 2512 cm^{-1} to 2513 cm^{-1} .

Sometimes in infrared absorption spectra also other bands were observed – 1367 cm^{-1} (sample S8), 2348 cm^{-1} (sample SA12), 2688 cm^{-1} (sample S8), 2594 cm^{-1} (sample S2), 2599 cm^{-1} (sample SA12), 2875 cm^{-1} (in all samples) and 2983 cm^{-1} (samples SA10, SO1, SO28, S2, S8). High-Mg calcite was identified only in sample SA12 (limestone of the Chelm Coquina Member), on the basis of infrared bands $V_1 + V_4 = 1800 \text{ cm}^{-1}$ and 2984 cm^{-1} (Pl. 15A). Dolomite was determined in two limestones of the St. Anne's Mountain Encrinite Member, in sample SA10 on the basis of bands 2360 cm^{-1} and 2610 cm^{-1} , and in SO1 – on the basis of bands 2385 cm^{-1} , 2360 cm^{-1} and 2610 cm^{-1} (Pl. 15 B) and in two limestones of the Chelm Coquina Member, in samples S2 – on the basis of band 2360 cm^{-1} and in S8 – on the basis of band $V_4 = 729 \text{ cm}^{-1}$ (Pl. 15C and 15D). Huntite was identified in the samples from the St. Anne's Mountain Encrinite Member (SO1 – Pl. 15 B) and the samples from the Chelm Coquina Member (SA12 – Pl. 15A and S2 – 15C). Huntite was determined based on the infrared bands of the values: 1555 cm^{-1} – in sample S2, 1561 cm^{-1} – in sample SA12 and 1562 cm^{-1} – in sample SO1 (Ramseyer et al., 1997; <http://ruff.info/Huntite>). Moreover, feldspars (samples SO28, SO1, SA10, SA12, S2), quartz (samples SO28, SA10, SA12) and kaolinite – (sample SO1) were identified (Stanienda, 2013a).

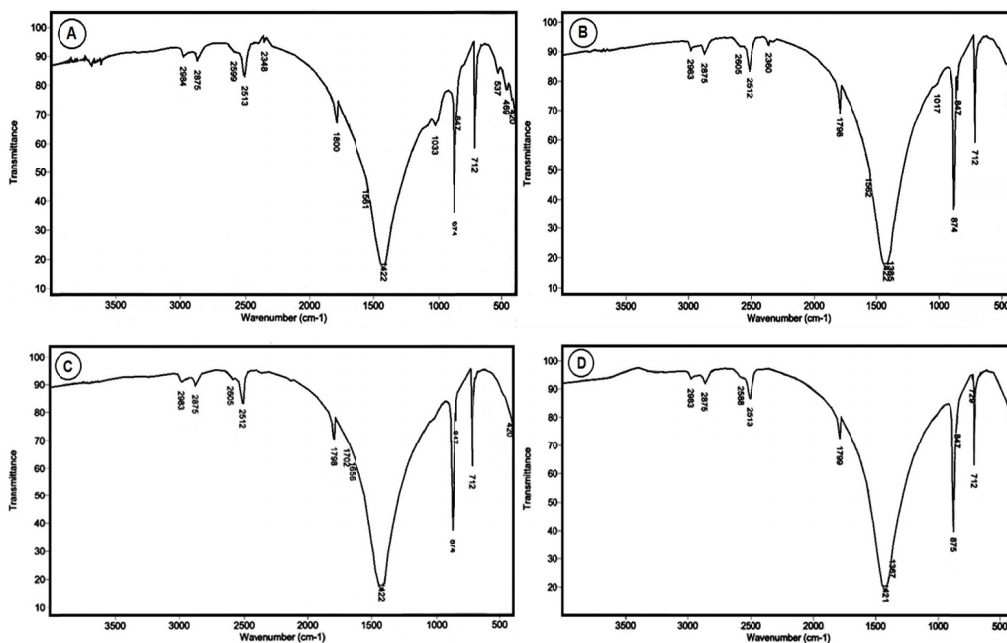


Plate 15. Infrared absorption spectra of limestone samples in the range from 400 to 4000 cm^{-1} .

A – Infrared absorption spectrum of the sample SA12 (Stanienda, 2013a); B – Infrared absorption spectrum of the sample SO1 (Stanienda, 2013a, b); C – Infrared absorption spectrum of the sample S2 (Stanienda, 2013a); D – Infrared absorption spectrum of the sample S8 (Stanienda, 2013a)

4. Discussion

4.1. Carbonate phases in limestones of the Terebratula Beds

The research results show that in limestones of the Terebratula Beds four carbonate phases were identified: low-Mg calcite, high-Mg calcite, dolomite and huntite. Low-Mg calcite and high-Mg calcite are usually mixed in groundmass of limestones poor in allochems or form micritic cement in limestones with bioclasts. Larger sparry low-Mg calcite grains are different in size (0.02-0.1 mm) and shape (irregular, oval, sometimes rhombohedral). In some areas of samples they form aggregates, sometimes fill in dissolution seams or cracks. Sparry xenomorphic low-Mg calcite grains could be treated as products of diagenetic processes- aggradation and recrystallization of micritic grains of primary carbonate material. Visible in thin sections crystals of calcite often form palisade neomorphic sparite which surrounds bioclasts. Dolomite forms euhedral, rhombohedral crystals. Some of them filled with iron minerals are pseudomorphs after dolomite. In thin sections also quartz, chalcedony, iron minerals (iron oxides and pyrite) and in some samples – clay minerals were determined. The results of X-ray diffraction, microprobe measurements and FTIR spectroscopy show that in all investigated limestones low-Mg calcite dominates. High-Mg calcite, dolomite and huntite also occur. High-Mg calcite was determined only in diffractograms of two samples: S2 and S5. Dolomite occurred in three samples: SO30, SA10, S5 and huntite – only in one sample S5. The results of X-ray indicate also the presence of ankerite (in samples SO1, SO28, SO30) and quartz (in samples SO1, SO30, S2, S5). According to FTIR results, high-Mg calcite is present only in rocks of the Chelm Coquina Member (sample SA12), dolomite – in rocks of the St. Anne's Mountain Encrinite Member (samples SA10, SO1) and in the rocks of the Chelm Coquina Member (samples S2, S8), huntite – in the rocks of the St. Anne's Mountain Encrinite Member (SO1) and the rocks of the Chelm Coquina Member (SA12, S2). The results of microprobe measurements show that the limestones of the Terebratula Beds are mainly built of low-Mg calcite but other carbonate phases were identified as well- high-Mg calcite, dolomite and huntite (Stanienda, 2013a, b). According to the results, the content of Mg in low-Mg calcite presents values below 3.5% and in high Mg-calcite, which was determined in the sample S2 – rock from the Chelm Coquina Member, it oscillates from 7.1 to 10.1%. The chemical formula of low-Mg calcite calculated on the basis of microprobe measurements results can be demonstrated as follows: $(Ca_{1-0.98}, Mg_{0-0.02})CO_3$ and that of high-Mg calcite as follows: $(Ca_{0.87-0.74}, Mg_{0.13-0.26})CO_3$ (Stanienda, 2013a). Dolomite occurred only in sample S2. Huntite was also identified only in this sample. The content of Mg in the dolomite of Terebratula Beds of limestone presents value 13.20%, which is similar to the stoichiometric value of Mg for this carbonate phase- 13.18 % (21.86% of MgO, 45.91% of $MgCO_3$). It indicates the presence of ordered dolomite in this rock, because non-stoichiometric, poorly ordered protodolomite is characterized by a lower than stoichiometric value of MgO in crystal (Morse & Mackenzie 1990; Boggs, 2010). The value of Mg content in huntite oscillates from 14.56 to 16.18%. It is a lower value than the stoichiometric one for this carbonate phase – 20.65% (34.25% of MgO, 71.93% of $MgCO_3$) (<http://truff.info/Huntite>). The decrease of Mg in primary huntite could be caused by removing Mg ions from huntite structure during diagenesis (probably calcitization?) (Stanienda, 2013a, b). Because of this, the calculated Mg/Ca ratio for huntite presents a value below 1.00 which is lower than the one for stoichiometric contents of Mg and Ca (it ranges between 2.04 and 3.85, with an average of 2.77) (Yavuz et al., 2006; Stanienda, 2013b).

The occurrence of Sr and Ba determined during microprobe measurements could indicate the presence of aragonite in primary carbonate material. Sr and Ba occur in aragonite skeletons and shells of sea organisms (Boggs, 2010; Fairchild et al., 2000). Because of its bigger ionic radius than the ionic radius of Ca, Sr enters more easily into the aragonite crystal structure, which is similar to strontianite, than into the calcite crystal structure. The ionic radius of Ba^{2+} is similar to the ionic radius of Sr^{2+} (Boggs, 2010). So Ba such as Sr could occur in aragonite. The study results also indicate the presence of a low amount of iron minerals (iron oxides and pyrite) as well as silicates and aluminosilicates in limestones of the Terebratula Beds from the area of Opole in Silesia. On the basis of the results obtained from measurements done by EDS and WDS methods the values of MgCO_3 content were calculated. These values, data from previous studies (Stanienda, 2013a, b) and the application of the Vegard's law which describes the empirical relationship between the crystal lattice parameter of a mixture and its components (Datta Roy & Das, 2000; Jacob et al., 2007; Lambregts & Frank, 2004; Melteig, 2016; Tompa et al., 2014) gave the opportunity to present the possible values of calcite phases cell parameters. With the increase in MgCO_3 content in high magnesium calcite the values of cell parameters – a_0 (Å) and c_0 (Å) drop (Zhang & Dave, 2010). When the amount of MgCO_3 is 22.7% (10.80% of MgO), the cell parameters of high-Mg calcite present general values as follows: $a_0 = 4.91 \text{ \AA}$, $c_0 = 16.65 \text{ \AA}$ and for the amount of MgCO_3 36.71% (17.48% of MgO) the cell parameters of this mineral present general values: $a_0 = 4.88 \text{ \AA}$, $c_0 = 16.45 \text{ \AA}$ (Zhang & Dave, 2010). Mg substitutions in crystals of high-Mg calcite cause a change of crystal cell structure of this mineral phase in comparison with low-Mg calcite crystal. It is connected with a difference in the size of ionic radius of Ca and ionic radius of Mg (Titiloye et al., 1998). On the basis of the MgO content, according to ICDD Card Index, a_0 and c_0 parameters were established. The values are as follows: $a_0 = 4.941 \text{ \AA}$, $c_0 = 16.854 \text{ \AA}$. They indicate the presence of high-Mg calcite in rocks of the Terebratula Beds, which is characterized by the content of MgO around 10.8%. According to literature data, the crystal structure of carbonate minerals rich in magnesium is as follows: protodolomite ($\text{Ca}_{0.5}\text{Mg}_{0.5}\text{CO}_3$; space group $R\bar{3}c$), ordered dolomite ($\text{Ca}_{0.5}\text{Mg}_{0.5}\text{CO}_3$; space group $R\bar{3}$), huntite ($\text{Ca}_{0.25}\text{Mg}_{0.75}\text{CO}_3$; space group $R32$) and magnesite (MgCO_3 ; space group $R\bar{3}c$) (Böttcher et al., 1997). The symmetry of high-Mg calcite crystal is rhombohedral with the space group $R\bar{3}c$ (Althoff, 1977; Paquette & Reeder, 1990). Dolomite of the Terebratula Beds limestones presents the stoichiometric value of MgCO_3 for dolomite. Its chemical formula is $(\text{Ca},\text{Mg})(\text{CO}_3)_2$. The content of Mg in dolomite chemical formula can be demonstrated as follows: $\text{Ca}_{0.5}\text{Mg}_{0.5}\text{CO}_3$. The results of the studies showed that the limestones of the Terebratula Beds also contain a low amount of huntite – magnesium and calcium carbonate with the chemical formula $\text{CaMg}_3[\text{CO}_3]_4$ (Dollase & Reeder, 1986). The content of Mg in its chemical formula can be demonstrated as follows: $\text{Ca}_{0.25}\text{Mg}_{0.75}\text{CO}_3$. According to the results, small differences in carbonate phases content were observed in each of three members of the Terebratula Beds. In rocks of each member low-Mg calcite dominates. The highest content of high-Mg calcite was determined in rocks from the Chelm Coquina Member. The increased amount of dolomite was determined in rocks from the St. Anne's Mountain Encrinite Member and these from the Chelm Coquina Member. Low content of huntite was identified only in rocks of the Chelm Coquina Member. Ankerite was determined in some samples of the Kamionek Marl Member and the St. Anne's Mountain Encrinite Member. In rocks from all members non-carbonate phases were determined (quartz, chalcedony, feldspars, clay minerals, iron oxides and pyrite). They dominate in the Kamionek Marl Member. Lower amounts were observed in rocks from the other two units. Analyzing the possibilities of carbonates formation it can be suspected that primary low-Mg calcite and high-Mg calcite which built

the first generation cement in the rocks the Terebratula Beds from the area of Opole Silesia were formed in the epicontinental Germanic Basin during direct crystallization from sea water at the same time as aragonite (early stage of diagenesis) (Szulc, 2000). The sources of Mg are usually sea waters but sometimes fresh waters as well. Mg could have also come from weathering land carbonate or silicate rocks. When delivered to sea water in a shelf zone, sometimes high-Mg calcite is formed (Mackenzie & Anderson, 2013). Some amounts of Mg could have come from sea organisms – shells and different parts of skeletons (Goffredo et al., 2012; Morse et al., 2006). Dolomite was probably formed in the mixing zone of the waters from the phreatic zone and salty sea waters during early constructive diagenesis (eogenetic stage of diagenesis) (Ali et al., 2010; Bodzioch, 2005; Szulc, 2000). The mosaic pseudospir (second generation cement) is the product of aggradation and recrystallization processes (mesogenetic stage of diagenesis) (Ali et al., 2010). Huntite was formed in the areas of the Germanic Basin in which diagenetic processes took place with the contribution of waters from the vadose zone (Deelman, 2011; Stanienda, 2013a, b). Non-carbonates are terrigenous apart from chalcedony and quartz which are products of silification processes (Bodzioch, 2005). Silification and dedolomitization happened during the telogenetic stage of diagenesis, when long-buried rocks were affected by processes associated with uplift and erosion (Ali et al., 2010).

4.2. Practical application of limestone with carbonate phases rich in magnesium

The data also present practical importance. Limestones are used as a sorbent in processes of flue gases desulfurization in power plants. Usually “pure” limestone with content of MgO <2% is applied. But analyzing the possibility of application of limestones including carbonate phases rich in magnesium, it can be said that these rocks may be a better sorbent than “pure” limestone built mainly of low-Mg calcite. This type of sorbent could be used especially applying dry method when coal combustion run in Fluidized Bed Reactor (Lysek, 1997, Nadziakiewicz & Janusz, 1999). Effectiveness of this method is 95%. In these method desulfurization process is going in bed composed of fluidized stream of air containing small particles of fly ash, sorbent and fuel. Two chemical reactions are going during dry desulfurization process, when limestone is used as a sorbent and three when dolomite is used (Lysek, 1997; Nadziakiewicz & Janusz, 1999) (Tab. 9).

TABLE 9

Chemical reactions going during desulfurization

No	Limestone is used as a sorbent		
1.	Desintegration of CaCO ₃	CaCO ₃ = CaO + CO ₂ (calcination)	[890°C]
2.	Reaction of joining SO ₂ by CaO. CaSO ₄ is formed	CaO + SO ₂ + 0,5 O ₂ = CaSO ₄	
Dolomite is used as a sorbent			
1.	Desintegration of dolomite	CaCO ₃ * MgCO ₃ = CaCO ₃ + MgCO ₃	
2.	Calcination of carbonates	MgCO ₃ = MgO + CO ₂ CaCO ₃ = CaO + CO ₂	[750°C] [890°C]
3.	Reaction of decarbonates with SO ₂	CaO + SO ₂ + 0,5 O ₂ = CaSO ₄ 2 MgO + SO ₂ + 0,5 O ₂ = MgSO ₄ + MgO	

Using dolomite as a sorbent for desulphurization of flue gases in power plants makes the effectiveness of the process better because the temperature of decarbonization of dolomite is lower than the decarbonization temperature of calcite, so the time of reaction of decarbonates with flue gases is longer. But because of the worse physical properties of dolomite (for instance – hardness) and the presence of periclase in product, which is formed during the reaction, dolomite is used very seldom as a sorbent for desulfurization of flue gases in power plants in Poland. So as it will be better to use limestone including apart of “pure” calcite also carbonates rich in magnesium than dolomite. The effectiveness of desulfurization process is higher with application of the limestone including carbonate phases rich in magnesium because decarbonization of these phases undergoes in lower temperatures than the decarbonization of “pure” calcite (low-Mg calcite). It is connected with a difference in the size of calcium and magnesium ions and the strength of ionic bonds. Substitution of magnesium in carbonate phases causes a decrease in ionic bond strength so the process of decarbonization of carbonate minerals occurs in lower temperatures. Lower temperatures of decarbonization of phases rich in magnesium cause earlier oxide secretion from carbonate minerals and because of it their earlier binding of sulfur oxides and REA gypsum formation. Thus the desulfurization process is more effective. Because of it the limestone which is built not only of low-Mg calcite but also of carbonate phases rich in magnesium, like high-Mg calcite, dolomite and huntite, could be a better sorbent than “pure” limestone built only of low-Mg calcite. The material which is formed during dry desulphurization includes many components (Lysek, 1997; Nadziakiewicz & Janusz, 1999) (Tab. 10). When “pure” limestone including below 2% of MgO is used as sorbent REA-gypsum is formed during desulfurization process. It is used especially in building construction and other branches of industry.

TABLE 10

Composition of desulfurization product

Type of desulfurization product	Composition
Fly ash	Fine grained material including grains smaller than 0,1 mm. It contains minerals and glassy substance. The most common minerals of fly ash: mullite (10-20%), quartz (4-15%), calcite (0,8-3,4%), hematite (2-9,5%), magnetite (0,9-12%), CaO (0,6-12%), periclase – MgO (2-3%), gypsum (1-2%). Heavy metals: As, Be, Cd, Cr, Co, Zn, Pb, Cu, Ni, V. Other chemical elements: ash: Al, Hg, Mn, Se, Tl.
Slag-coarse-grained material	Its mineral composition is similar to components of fly ash.
Chemical compounds	Products of chemical reactions between SO ₂ and CaO: CaSO ₂ *2H ₂ O (gypsum), anhydrite (CaSO ₂), CaSO ₃ , CaO, MgO (periclase – when dolomite is used as a sorbent), CaCl ₂ , aluminosilicates of Ca, K and Mg, Ca ₆ Al ₂ [(OH) ₄ SO ₄] ₃ *24H ₂ O (ettringite), Fe ₂ O ₃ (magnetite), FeS (pirotine) and particles of sorbent (CaCO ₃) (Ikavalko et al., 1995; Kanafek & Fojcik, 1998; Sanders et al., 1995).

But it must be for each application adapted. If limestone including carbonate phases rich in Mg (especially high-Mg calcite) is used as a sorbent the product of reaction will include also magnesium phases apart from gypsum and anhydrite like in case of dolomite application. So as it will be necessary to determine the possibilities of application the product which includes

magnesium sulfates and periclase. Desulfurization of flue gases is very important, because in many Polish power plants and also power plants in other countries of the world coal is used as a main energy resource. There is often an impurity of sulfur in coal so it is necessary to use desulfurization of flue gases which are emitted during coal combustion to reduce the emission of sulfur oxides into the atmosphere. It allow to reduce the air contamination which occur during energy production applying coal as the energy resource. However, the use of sorbent containing high-Mg calcite, dolomite and huntite may cause the desulfurization process significantly more energy-consuming than with a use of limestone built of “pure” calcite. Moreover, application a sorbent which contains carbonate phases with magnesium may cause higher costs due to severe corrosion of equipment in the system by the presence of the desulfurization products soluble in water vapor exhaust magnesium sulfate. It must therefore be carefully analyzed the amount of carbonate phases with magnesium, present in the sorbent, and their type and moreover, the type of desulfurization method which is applied in power plant before making a decision about applying sorbent including magnesium carbonates for desulfurization of flue gases.

5. Conclusions

The results of executed analyses indicate the presence of four carbonate phases with different content of Mg in the rocks of the Terebratula Beds from the area of Opole Silesia: low-Mg calcite, high-Mg calcite, dolomite and huntite. Micritic grains of high-Mg calcite mixed with micritic grains of low-Mg calcite build the groundmass or cement in organic limestones. Mixed dolomite and huntite form euhedral crystals, rhombohedral in shape. Some of them are filled with iron minerals. They are pseudomorphs after dolomite. X-ray diffraction allow to determine apart low-Mg calcite and dolomite also high-Mg calcite (in two samples – S2 and S5) and huntite (only in one sample – S5). Moreover, in three samples (SO1, SO28, SO30) ankerite was observed and in some samples – quartz (in SO1, SO30, S5). The results of microprobe measurements confirmed the presence of four carbonate phases different in Mg content: low-Mg calcite, high-Mg calcite, dolomite and huntite. The content of Mg in low-Mg calcite presents values below 3.5%. So the chemical formula of this mineral can be demonstrated as follows: $(Ca_{1-0.98}, Mg_{0-0.02})CO_3$. In high Mg-calcite the Mg content varies in the range from 7.10 to 10.10%, so as its chemical formula can be demonstrated as follows: $(Ca_{0.87-0.74}, Mg_{0.13-0.26})CO_3$. The content of Mg in dolomite of Terebratula limestone presents value 13.20%. Because it's similarity to the stoichiometric value of Mg for this carbonate phase this phase could be treated as ordered dolomite. The value of Mg content in huntite varies in the range from 14.56 to 16.18%. It is lower than the stoichiometric value for this carbonate phase – 20.65%. The decrease in Mg in this phase could be caused by removing Mg ions from the crystal structure during diagenesis. The results of microprobe measurements indicate the presence of a low amount of iron minerals (ankerite/iron oxides/pyrite) and also silicates and aluminosilicates in limestones of the Terebratula Beds from the area of Opole Silesia. Results of FTIR Spectroscopy also confirmed the presence of four carbonate phases different in magnesium content. According to the results of studies it can be said that primary low-Mg calcite and high-Mg calcite of the Terebratula Beds from the area of Opole Silesia were formed in the epicontinental germanic basin during crystallization from sea water at the same time as aragonite (the eogenetic stage of diagenesis). The conditions of sea water, especially higher salinity,

and diagenetic processes might have influenced the preservation of high-Mg calcite (unstable carbonate phase) in Muschelkalk limestones of the Polish part of the Germanic basin. Sparry calcite was formed during advanced diagenesis. Dolomite was probably formed in the mixing zone of the waters from the phreatic zone and salty sea waters during the early constructive diagenesis (the eogenetic stage). Pseudomorphs after dolomite are products of dedolomitization processes which happened during the telogenetic stage of diagenesis. Huntite was formed in the area of the Germanic Basin in which diagenetic processes took place with the contribution of waters from the vadose zone. Non-carbonate minerals are terrigenous apart from quartz and chalcedony (products of silification). The results show that there is no big differences in carbonate phases content in rocks from three members of the Terebratula Beds. In rocks from each member low-Mg calcite dominates. The highest content of high-Mg calcite was determined in rocks from the Chelm Coquina Member. The increased amount of dolomite was determined in rocks from Kamionek Marl Member, rocks from St. Anne's Mountain Encrinite Member and these from the Chelm Coquina Member. Low content of huntite was identified in rocks from the St. Anne's Mountain Encrinite Member and the samples from the Chelm Coquina Member. Moreover, ankerite was determined in some samples of the Kamionek Marl Member and the St. Anne's Mountain Encrinite Member. Non-carbonate phases dominate in the Kamionek Marl Member, lower amounts were determined in rocks of from the other two members.

The research results indicate the possibility of application the limestones with magnesium which build the Terebratula Beds in desulfurization of flue gases in power plants. Substitution of Mg in carbonate phases causes a decrease in ionic bond strength so decarbonization carbonates rich in Mg decarbonization of carbonate minerals run in lower temperatures, and sulfur oxides are earlier caught by calcium and magnesium oxides what makes the desulfurization process more effective. So as it is important knowledge because allow to consider the application of limestone including phases rich in magnesium in desulfurization of flue gases instead of "pure" limestone build mainly of low-Mg calcite or calcite without substitutions. However the application of sorbent which contains carbonate phases with magnesium is more may cause the process significantly more energy-consuming and may increase the costs due to severe corrosion of equipment in the system. But limestone including carbonate phases rich in magnesium is better sorbent than dolomite, because of higher hardness of dolomite and higher content of magnesium sulfates and periclase in post-reaction product which is more difficult to use than product built mainly of calcium phases with lower addition of magnesium minerals, especially periclase which is an inert material and usually does not react with other substances.

References

- Ali S.A., Clark W.J., Moore W.R., Dribus J.R., 2010. *Diagenesis and reservoir quality*. Oilfield Review 22, 2, 14-27.
- Althoff P.L., 1977. *Structural refinements of dolomite and a magnesian calcite and implications for dolomite formation in the marine environment*. American Mineralogist 62, 772-783.
- Atay H.Y., Çelik E., 2010. *Use of Turkish Huntite/Hydromagnesite Mineral in Plastic Materials as a Flame Retardant*. Polymer Composites, 1691-1700.
- Bodzioch A., 2005. *Biogeochemical diagenesis of the Lower Muschelkalk of Opole region*. Adam Mickiewicz University Press, Poznań, Geologia, 17.
- Boggs S. Jr., 2010. *Petrology of sedimentary rocks*. Second Edition, Cambridge University Press.

- Böttcher M.E., Gehlken P.L., Steele F.D., 1997. *Characterization of inorganic and biogenic magnesian calcites by Fourier Transform infrared spectroscopy*. Solid State Ionics 101-103, 1379-1385.
- Datta Roy S., Das S.K., 2000. *A green function estimation of correction to Vegard's law for isovalent substitutional defects in alkali halide crystals*. Acta Physica Polonica A 97, 4, 671-679.
- Deelman J.C., 2011. Low-temperature formation of dolomite and magnesite. Available: http://www.jedeelman.demon.nl/dolomite/files/13_Chapter6.pdf.
- Dollase W.A., Reeder R.J., 1986. *Crystal structure refinement of huntite, CaMg₃[CO₃]₄, with X-ray powder data*. American Mineralogist 71, 163-166.
- Fairchild I.J., Borsato A., Tooth A.F., Frisia S., Hawkesworth C.J., Huang Y., Mc Dermott F., Spiro B., 2000. *Controls on trace element (Sr-Mg) composition of carbonate cave waters: implication for speleothem climatic records*. Chemical Geology 166, 255-269.
- Flügel E., 2004. *Microfacies in carbonate Rocks*. Analysis, Interpretation and Application. Springer-Verlag Berlin Heidelberg.
- Goffredo S., Caroselli E., Mezzo F., Laiolo L., Vergni P., Pasquini L., Levy O., Zaccanti F., Tribollet A., Dubinsky Z., Falini G., 2012. *The puzzling presence of calcite in skeletons of modern solitary corals from the Mediterranean Sea*. Geochimica et Cosmochimica Acta 85, 187-199.
- Ikavalko E., Laitinen T., Parkka M., Ylirokanen I., 1995. *Intercomparizon of trace-element determination in samples from a Coal Fired Power-Plant*. Int. J. Environ. Anal. Chem. 61, 3, 207-224.
- Jacob K.T., Shubhra Raj, Ranesh L., 2007. *Vegard's law: A fundamental relation or an approximation?* International Journal of Materials Research 98, 9, 1-13.
- Kanafek J., Fojcik E., 1998. *Wykorzystanie popiołów lotnych w górnictwie- aspekty techniczne*. Ochrona Środowiska Prawo i Polityka 1, 11, 23-34.
- Lambregts M.J., Frank S., 2004. *Application of Vegard's law to mixed cation sodalites: a simple method for determining the stoichiometry*. Talanta 62, 627-630.
- Lysek N., 1997. *Sorbenty do odsiarczania gazów. Produkcja i zastosowanie*. Published in Kraków.
- Mackenzie F.T., Andersson A.J., 2013. *The Marine carbon system and ocean acidification during Phanerozoic Time*. Geochemical Perspectives 2, 1.
- Melteig H.E., 2016. *Cation substitution in two coccolithophore species. Can coccolithophores be used in material synthesis?* University Print Center, University of Oslo.
- Morse J.W., Andersson A.J., Mackenzie F.T., 2006. *Initial responses of carbonate-rich shelf sediments to rising atmospheric pCO₂ and "ocean acidification": Role of high Mg-calcites*. Geochimica et Cosmochimica Acta 70, 5814-5830.
- Nadziakiewicz J., Janusz M., 1999. *Mitigation of sulphur dioxide emission in power plant boilers*. Gospodarka Paliwami i Energią 12, 12-15.
- Niedźwiedzki R., 2000. *Litostratygrafia formacji górażdżańskiej i formacji dziewkowickiej na Śląsku Opolskim*. Prace Geologiczno-Mineralogiczne Uniwersytetu Wrocławskiego, LXXI, Wrocław.
- Paquette J., Reeder R.J., 1990. *Single-crystal X-ray structure refinements of two biogenic magnesian calcite crystals*. American Mineralogist 75, 1151-1158.
- Ramseyer K., Miano T.M., D'Orazio V., Wildberger A., Wagner T., Geister J., 1997. *Nature and origin of organic matter in carbonates from speleothems, marine cements and coral skeletons*. Org. Geochem. 26 (5/6), 361-378.
- Sanders J.F., Keener T.C., Wang J., 1995. *Heated fly ash, hydrate lime slurries for SO₂ removal in spray drayer absorbers*. Industrial & Engineering Chemistry Research 1, 1.
- Smyth J.R., Ahrens T.J., 1997. *The crystal structure of calcite III*. Geophysical Research Letters 24, 13, 1595-1598.
- Stanienda K., 2011. *Effects of dolomitization processes in the Triassic limestone of Tarnów Opolski Deposit*. Monografia, Silesian University of Technology Press, Gliwice.
- Stanienda K., Kokowska-Pawłowska M., Marcisz M., 2011. *Geotouristic qualities of Chelm Hummock Triassic limestone*. Kwartalnik Górnictwo i Geologia 6, 3, 169-181.
- Stanienda K., 2013a. *Diagenesis of the Triassic limestone from the Opole Silesia in the aspect of magnesian calcite presence*. Monografia, Silesian University of Technology Press; Gliwice.
- Stanienda K., 2013b. *Huntite in the Triassic limestones of Opolski Silesia*. Mineral Resources Management, IGSMiE PAN, Kraków 29 (3), 79-98.

Szulc J., 2000. *Middle Triassic evolution of the Northern Peri-Tethys area is influenced by early opening of the Tethys Ocean*. *Annales Societatis Geologorum Poloniae* 70, 1-48.

Titiloye J.O., De Leeuw N.H., Parker S.C., 1998 *Atomistic simulation of the differences between calcite and dolomite surfaces*. *Geochim. Et Cosmochim. Acta* 62, 15, 2637-2641.

Tompa E., Nyirő-Kósa I., Rostási A., Cserny T., Pösfai M., 2014. *Distribution and composition of Mg-calcite and dolomite in the water and sediments of Lake Balaton*. *Central European Geology* 57/2, 113-136.

Yavuz F., Kırkoğlu M.S., Özden G., 2006. *The occurrence and geochemistry of huntite from Neogene lacustrine sediments of the Yalvaç-Yarıkkaya Basin, Isparta, Turkey*. *N. Jb. Miner. Abh.* 182/2, 201-212.

Zahng Y., Dave R.A., 2000. *Influence of Mg²⁺ on the kinetics of calcite crystal morphology*. *Chemical Geology* 163, 129-138.

<http://rruff.info/Huntite>

<http://www.webmineral.com/data/Dolomite.shtml>